



ORIGINAL ARTICLE

Synthesis, characterization and self-assembly of novel fluorescent alkoxy-substituted 1, 4-diarylated 1, 2, 3-triazoles organogelators



Salhah D. Al-Qahtani ^a, Razan M. Snari ^b, Abrar Bayazeed ^b, Rua B. Alnoman ^c,
Aisha Hossan ^d, Amerah Alsoliemy ^b, Nashwa M. El-Metwaly ^{b,e,*}

^a Department of Chemistry, College of Science, Princess Nourah bint Abdulrahman University, P.O. Box 84428, Riyadh 11671, Saudi Arabia

^b Department of Chemistry, Faculty of Applied Science, Umm-Al-Qura University, Makkah 24230, Saudi Arabia

^c Department of Chemistry, College of Science, Taibah University, Madinah, P.O. Box 344, Saudi Arabia

^d Chemistry Department, Faculty of science, King Khalid University, Abha, Saudi Arabia

^e Department of Chemistry, Faculty of Science, Mansoura University, El-Gomhoria Street, 35516, Egypt

Received 4 January 2022; accepted 26 March 2022

Available online 29 March 2022

KEYWORDS

CuAAC;
1,2,3-Triazole;
Fluorescence;
Self-assembly;
Nanofibers

Abstract Novel organogelators based on fluorescent alkoxy-substituted 1,4-diarylated 1, 2, 3-triazoles are reported. The findings monitored in the current study promoted the development of inventive compacted supramolecular architectures generated by self-assembly of the prepared triazole-based organogelators. The synthesis, characterization and gelation properties of the current novel alkoxy-substituted 1,4-diarylated 1, 2, 3-triazole arms were described. The synthesis procedures were accomplished by using Cu-catalyzed azide-alkyne cycloaddition (CuAAC) of alkoxy-substituted aryl azide with aryl bearing terminal alkyne substituents and alkoxy chains of different lengths. The alkoxy-substituted 1, 4-diarylated 1, 2, 3-triazole derivatives bearing different alkoxy chains were characterized by FTIR, ¹H/¹³C NMR, and elemental analysis. The 1, 4-diarylated 1, 2, 3-triazoles with longer alkoxy terminal groups demonstrated improved gelation properties compared to those with shorter alkoxy terminals. The morphologies of the self-assembled alkoxy-substituted 1, 4-diarylated 1, 2, 3-triazoles were investigated using scanning electron microscopy (SEM), which demonstrated arrangements of highly ordered nanofibers, forced by π -stacks and van der Waals interactions. The antibacterial activity and cytotoxicity of the newly

* Corresponding author at: Department of Chemistry, Faculty of Applied Science, Umm-Al-Qura University, Makkah 24230, Saudi Arabia.
E-mail addresses: n_elmetwaly00@yahoo.com, nmmohamed@uqu.edu.sa (N.M. El-Metwaly).

Peer review under responsibility of King Saud University.



synthesized triazoles was investigated to verify the potential use of the present triazole gelators for a variety of applications, such as drug delivery.

© 2022 The Author(s). Published by Elsevier B.V. on behalf of King Saud University. This is an open access article under the CC BY-NC-ND license (<http://creativecommons.org/licenses/by-nc-nd/4.0/>).

1. Introduction

Because of their thermoreversibility, chemical sensitivity, and variety of macroscale structures, low molecular mass organogels are becoming more important. Organogels have been utilized for a variety of fields, including biological, cosmetic, and foodstuff applications (Agarwal et al., 2020; Goyal et al., 2020; Zhang et al., 2021). There has been a lot of interest in the self-assembling small organic molecules or gelator subsets, which can entrap tolerable volumes of solvents giving them novel properties useful for various applications. The design and formation of self-assembled structures can display distinctive optoelectronic features, like enhanced fluorescence and high charge transfer (Bhardwaj and Ballabh, 2022; Mandegani et al., 2020). A supramolecular gel is defined as a soft material composed of a solid-like fluid with a viscoelastic performance owing to the presence of a gelator able to self-assemble into 3D ordered networks. Those networks can be formed in various shapes, such as nanofibers, nanorods and nanosheets (Lakdusinghe et al., 2021). Self-assembling gelators have become of interest in the fields of catalysis, tissue engineering, drug self-delivery, pollutants removal, sensing, and data storage (Esposito et al., 2018; Zeng et al., 2021; Zhang et al., 2020). The self-assembly attraction forces could be assigned to phase transition, physical bonding, crosslinking and/or chemical bond formation (Naim et al., 2021). Recently, the distinct capacity of small molecular gelators to hold liquids by non-covalent bond formation, like van der Waals forces, H-bonding, and π -stacks, has received substantial attention (Morris et al., 2021; Raymond et al., 2019; Yang et al., 2017). The molecules of an organogelator can be self-assembled into highly ordered supramolecular nanofibers without converting to dense structures. Some of the many uses for low molecular mass organogels include the creation of nanoporous materials, improvement of rheological characteristics in cosmetics, foodstuff, sensors and biosensors, drug delivery, tissue engineering, removal of pollutants, and polymer crystal nucleating agents (Reddy et al., 2017; Vishnevetskii et al., 2020; Wang et al., 2018).

In spite of the fact that the 1, 2, 3-triazole heterocycle itself does not exist in nature, it has been used as a crucial skeleton in a broad variety of biological activities, like anticancer and anti-HIV (Fernandes et al., 2019; Sharma et al., 2021; Zhang et al., 2019). The electron-deficiency monitored in 1, 2, 3-triazoles has made them excellent candidates for a diversity of technical applications, like organogels and liquid crystals. Organogelators with a 1, 2, 3-triazole moiety have lately gained a lot of attention because of their appealing chemical and physical properties. There are several ways to synthesize the 1, 2, 3-triazole heterocycle, such as the most common being Cu-assisted alkyne-azide cycloaddition (CuAAC) chemistry (Gholampour et al., 2019; Ross et al., 2021; van Hilst et al., 2018). Many studies have shown that the location of the 1, 2, 3-triazole heterocycle in the rigid core and type of substituents may have a substantial impact on gelation characteristics. Chemical stability, aromaticity, and hydrogen bonding acceptor ability are all strong features of the 1, 2, 3-triazole heterocycle containing derivatives. The presence of a heterocyclic moiety results in increasing the dipole and dielectric anisotropy, thus providing polar molecular aggregates by creating electrostatic and supramolecular structure-dependent attraction forces between the molecular units (Horsten et al., 2021; Gu et al., 2020; Güzel, 2019; Xu et al., 2018; Yang et al., 2019; Zych et al., 2019).

Only limited studies were reported on the development of fluorescent organogelators based on alkoxy-substituted 1, 4-diarylated 1, 2, 3-triazoles (Díaz et al., 2006; Ghosh and Panja, 2015; Huang et al., 2018; Huang et al., 2015; Tautz et al., 2019; Sharma et al., 2021).

Despite the fact that alkoxy-substituted 1, 4-diarylated 1, 2, 3-triazoles have played a key role in recent breakthroughs such as optoelectronics (Tao et al., 2010; Wu and Chen, 2010), very little reports of low molecular mass organogels based on triazoles have been reported yet. However, induced illumination during aggregation became the subject of recent investigations (Tang et al., 2009). Interesting work has been done regarding observing switching behavior to induced fluorescence emission after self-assembly of thin film. In addition, solid one-dimensional aggregations of helical nanofiber exhibit induced light emission by confining the possible internal bond rotations in solution. Although luminescent 3D supramolecular network gels are scarce, photo-responsive organogels are of interest for their potential application in biomaterials, optoelectronic devices, switches and sensors (Sun et al., 2017).

In this content, fluorescent triazole organogels based on rigid bis(triazole)aryl core and terminal flexible alkoxy chains have been reported. Novel fluorescent alkoxy-substituted 1, 4-diarylated 1, 2, 3-triazole organogelators with potential optoelectronic applications were synthesized, characterized, and self-assembled. CuAAC of alkoxy-substituted aryl azides with an aryl compound containing terminal alkyne groups and lengthy alkoxy side-chains was employed to provide the corresponding alkoxy-substituted 1, 4-diarylated 1, 2, 3-triazole organogelators. This led to the formation of a rigid, extended and conjugate bis(triazole)aryl core with strong light emission. Those alkoxy-substituted 1, 4-diarylated 1, 2, 3-triazoles with different alkoxy chain lengths were detected to display emission in the ultraviolet range of the electromagnetic spectrum. As a result, they could be reported as appropriate materials for lower energy consumption electronic displays particularly in portable displays (Alsoliemy et al., 2021; Oh et al., 2021). The gelation and supramolecular properties of the alkoxy-substituted 1, 4-diarylated 1, 2, 3-triazole derivatives were investigated in various solvents. The antimicrobial performance and cytotoxicity of alkoxy-substituted 1, 4-diarylated 1, 2, 3-triazole **3a-c** were studied. SEM was utilized to explore the nanostructured morphologies of self-assembled fluorescent organogels.

2. Experimental details

2.1. Materials and methods

Differential Scan Calorimetry (DSC; TA 2920) was used to measure the melting points. The $^1\text{H}/^{13}\text{C}$ NMR spectral analysis was performed on Bruker Avance 400 MHz. Perkin-Elmer 2400 (Norwalk, USA) was used to determine the elemental analysis. An Ultraviolet-Agilent from Cary Series was used to conduct the UV/Vis absorption spectra. The fluorescence quantum yields (Φ) and fluorescence spectral analysis were investigated by VARIAN CARY ECLIPSE. The fluorescence quantum yields (Φ) were determined using solutions of rhodamine 6G ($\Phi_r = 0.95$) and rhodamine 101 ($\Phi_r = 0.96$) in absolute ethanol as quantum yield standards. FT-IR Bruker Vectra 33 was used to get infrared spectra. A Quanta FEG 250 apparatus was used for the scanning electron microscopy (SEM) examination. In this experiment, we prepared an organogel in *n*-octanol, which was then air-dried on a clean glass slide. The gold-coated xerogel was exposed to annealing overnight at 45 °C. Unless otherwise stated, all materials used in the experiments were from Sigma-Aldrich and Merck (Egypt).

Compounds **1** (1,3 dialkoxy 4,6 diethynylbenzene) and **2** (5 azido 1,3 dialkoxybenzene) were synthesized in accordance with previous procedures (Afzali et al., 2021; Fakhruddin et al., 2021). Thin layer chromatography was utilized to observe the progress of reactions using aluminium-backed plate loaded with a coating of silica gel 60 under an ultraviolet lamp (UV₂₅₄). Silica gel 60 was applied to purify the synthesized compounds by flash column chromatography.

2.2. Gelation procedure

Compounds **3a-c** were dissolved in the specified solvents and heated at boiling point in a closed glass vial to generate a transparent solution, and subjected to cooling to ambient temperature to create gels. In 15–25 min, the gels formed relying on the organogelator concentration and the length of the aliphatic chain. The gel formation was confirmed by the “stable-to-inversion” approach as indicated by the solvent disappearance in the inverted vial. The reversibility was examined by heating (2 °C/min) the organogel-containing glass vial placed topsy-turvy in an oil bath. The temperature at which the gel collapses is reported as the gel melting point. The above procedures were repeated to designate a good reversibility.

2.3. Cytotoxicity assay

BJ1 skin fibroblast cells were used to conduct the cytotoxicity experiment *in vitro* following the previously established MTT proliferation technique (Abumelha et al., 2020).

2.4. Antibacterial activity

The antibacterial properties of the synthesized triazoles were explored against *S. aureus* and *E. coli* under AATCC (100:1999) (Aldalbahi et al., 2021).

2.5. Synthesis procedures

2.6. General synthesis of triazoles 3a-c

A mixture of diethynyl **1** (1 mmol), azido compound **2** (2 mmol), TBTA (tris((1-benzyl-4-triazolyl)methyl)amine; 0.1 mmol), sodium ascorbate (0.2 mmol) was dissolved in a mixture of distilled water:*t*-BuOH:CH₂Cl₂ (1:2:8) under argon atmosphere. Copper(II) sulfate (CuSO₄·5H₂O; 0.1 mmol) was then added to the mixture, followed with stirring under ambient conditions for 22 h. The reaction system was covered with aluminum foil to ensure that the reaction occurs in the dark. After complete consumption of alkyne, the mixture was diluted with dichloromethane. The organic layer was then subjected to extraction with dichloromethane, three times washing with aqueous brine. The dichloromethane solution was dried on magnesium sulfate (anhydrous), filtered off under vacuum, and finally dichloromethane was evaporated using a rotary evaporator. The solid product was subjected to column chromatography (ethyl acetate/ether 2/7).

Tetrahexyl-5, 5'-(4, 4'-(4, 6-bis(hexyloxy)-1, 3-phenylene)-bis(1*H*-1,2,3-triazole-4, 1-diyl))diiso-phthalate **3a**.

Prepared from **1** (326 mg, 1 mmol), azido compound **2a** (750 mg, 2 mmol), TBTA (tris((1-benzyl-4-triazolyl)methyl)

amine; 53 mg, 0.1 mmol), sodium ascorbate (40 mg, 0.2 mmol) and copper(II) sulfate (16 mg, 0.1 mmol). Prepared as a white powder with 88% (947 mg) yield; mp 191–192 °C; ¹H NMR (400 MHz; CDCl₃): 9.46 (s, 1H), 8.84 (s, 2H), 8.78 (s, 4H), 8.63 (s, 2H), 6.72 (s, 1H), 4.43 (t, *J* = 6.02 Hz, 8H), 4.20 (t, *J* = 6.11 Hz, 4H), 1.89 (m, 4H), 1.83 (m, 8H), 1.28–1.59 (m, 36H), 0.91 (t, *J* = 4.77 Hz, 18H); ¹³C NMR (400 MHz; CDCl₃): 165.85, 157.59, 145.73, 138.80, 133.86, 129.93, 128.64, 125.85, 119.72, 112.80, 97.47, 79.75, 66.20, 32.94, 31.567, 29.72, 29.36, 28.80, 26.10, 22.54, 14.20; IR (ν/cm⁻¹): 3065 (C-H aryl stretch), 2917 (CH alkyl asymmetric stretching), 2847 (CH alkyl stretch), 1731 (C = O stretch), 1589 (C = N), 1503 (C = C aryl bend), 1330 (C-O), 1188 (CH₂ alkyl bending), 1122 (CH₃ alkyl bending), 862 (C-H aryl bending), 723 (CH₂ alkyl bending rocking); Elemental analysis of C₆₂H₈₈N₆O₁₀ (1076.66): C 69.12, H 8.23, N 7.80; Found: 68.96, H 8.15, N 7.71.

Tetranonyl-5, 5'-(4, 4'-(4, 6-bis(hexyloxy)-1, 3-phenylene)-bis(1*H*-1,2,3-triazole-4, 1-diyl))diiso-phthalate **3b**.

Prepared from **1** (326 mg, 1 mmol), azido compound **2b** (918 mg, 2 mmol), TBTA (tris((1-benzyl-4-triazolyl)methyl)amine; 53 mg, 0.1 mmol), sodium ascorbate (40 mg, 0.2 mmol) and copper(II) sulfate (16 mg, 0.1 mmol). Prepared as a white powder with 81% (1.05 g) yield; mp 165–167 °C; ¹H NMR (400 MHz; CDCl₃): 9.41 (s, 1H), 8.80 (s, 2H), 8.76 (s, 4H), 8.58 (s, 2H), 6.70 (s, 1H), 4.39 (t, *J* = 6.18 Hz, 8H), 4.22 (t, *J* = 6.25 Hz, 4H), 1.88 (m, 4H), 1.85 (m, 8H), 1.25–1.67 (m, 60H), 0.92 (t, *J* = 4.81 Hz, 18H); ¹³C NMR (400 MHz; CDCl₃): 165.76, 157.64, 146.68, 139.79, 133.83, 129.78, 126.39, 123.72, 119.45, 110.74, 96.18, 69.73, 66.02, 31.91, 30.38, 29.77, 29.31, 29.21, 28.77, 25.87, 23.65, 22.28, 14.27; IR (ν/cm⁻¹): 3069 (C-H aryl stretch), 2918 (CH alkyl asymmetric stretch), 2850 (CH alkyl symmetric stretching), 1729 (C = O stretch), 1582 (C = N), 1508 (C = C aryl bend), 1337 (C-O), 1191 (CH₂ alkyl bend), 1125 (CH₃ alkyl bend), 867 (CH aryl bend), 728 (CH₂ alkyl bending rocking); Elemental analysis of C₇₄H₁₁₂N₆O₁₀ (1244.84): C 71.35, H 9.06, N 6.75; Found: C 71.48, H 9.15, N 6.83.

Tetradodecyl-5, 5'-(4, 4'-(4, 6-bis(hexyloxy)-1, 3-phenylene)-bis(1*H*-1,2,3-triazole-4, 1-diyl)) diiso-phthalate **3c**.

Prepared from **1** (326 mg, 1 mmol), azido compound **2c** (1.09 g, 2 mmol), TBTA (tris((1-benzyl-4-triazolyl)methyl)amine; 53 mg, 0.1 mmol), sodium ascorbate (40 mg, 0.2 mmol) and copper(II) sulfate (16 mg, 0.1 mmol). Prepared as a white powder with 78% (1.10 g) yield; mp 128–130 °C; ¹H NMR (400 MHz; CDCl₃): 9.45 (s, 1H), 8.80 (s, 2H), 8.79 (s, 4H), 8.62 (s, 2H), 6.71 (s, 1H), 4.37 (t, *J* = 6.28 Hz, 8H), 4.19 (t, *J* = 6.35 Hz, 4H), 1.86 (m, 4H), 1.84 (m, 8 H), 1.31–1.57 (m, 84H), 0.90 (t, *J* = 4.88 Hz, 18H); ¹³C NMR (400 MHz; CDCl₃): 165.26, 157.58, 145.84, 138.51, 133.45, 129.70, 127.61, 124.40, 119.60, 111.74, 96.38, 68.66, 66.81, 31.72, 31.20, 29.80, 29.68, 29.41, 29.26, 28.60, 26.77, 26.26, 22.64, 22.35, 14.11, 13.75; IR (ν/cm⁻¹): 3070 (CH aryl stretch), 2919 (CH alkyl stretch), 2851 (CH alkyl stretch), 1733 (C = O stretch), 1586 (C = N), 1501 (C = C aryl bend), 1328 (C-O), 1182 (CH₂ alkyl bending), 1116 (CH₃ alkyl bending), 858 (C-H aryl bending), 725 (CH₂ alkyl bending rocking); Elemental analysis of C₈₆H₁₃₆N₆O₁₀ (1413.03): C 73.05, H 9.69, N 5.94; Found: C 72.91, H 9.78, N 6.07.

3. Results and discussion

3.1. Synthesis and characterization

The major aim of the present research work was to prepare new fluorescent alkoxy-substituted 1, 4-diarylated 1, 2, 3-triazole gelators. The diethynyl compound **1** (1,3 dialkoxy 4,6 diethynylbenzene) and azido compound **2** (5 azido 1,3 dialkoxybenzene) compounds were synthesized in accordance with previous procedures (Afzali et al., 2021; Fakhrutdinov et al., 2021). As depicted in Scheme 1, alkoxy-substituted 1, 4-diarylated 1, 2, 3-triazoles (**3a**, **3b** and **3c**) were synthesized in relatively high yields using Cu(I)-catalyzed alkyne-azide cycloaddition (CuAAC) of compound **1** comprising two terminal alkyne groups and two terminal alkoxy substituents with 5 azido 1,3 dialkoxybenzene **2** with different alkoxy chain lengths. $^1\text{H}/^{13}\text{C}$ NMR, FTIR, and elemental analysis were used to prove the molecular structures of the novel compounds **3a-c**. ^1H NMR spectra of compound **3a-c** exhibited distinct signals for the alkoxy chain substituents ranging from ~ 0.90 to ~ 4.43 ppm. The symmetrical CH peaks of the 1, 2, 3-triazole heterocyclic rings were monitored to downfield shift at ~ 8.50 ppm. The ^{13}C NMR spectra of **3a-c** displayed 1, 2, 3-triazole C-H signal at ~ 145 ppm. The infrared spectra of **3a-c** showed strong absorbance peaks of the alkoxy groups at ~ 2920 and ~ 2850 cm^{-1} .

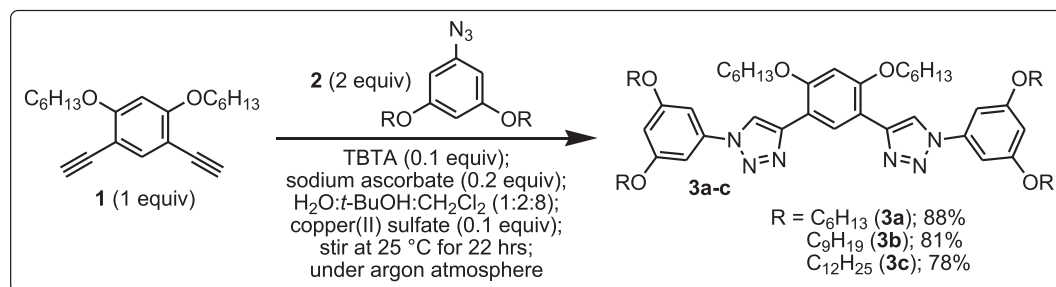
3.2. Photophysical properties

A stimuli-responsive chemical or product has the ability to vary its absorbance or emission spectra responding to external stimuli, like heat and/or light (Mellerup and Wang, 2019; Moulin et al., 2020; Rastogi and Kandasubramanian, 2019). Some selected solvents were used to study the UV-Vis absorption and fluorescence properties of the current alkoxy-substituted 1, 4-diarylated 1, 2, 3-triazole compounds as shown in Table 1. Both absorbance and fluorescence maxima of the alkoxy-substituted 1, 4-diarylated 1, 2, 3-triazole derivatives were reported in a range of solvents, including n-propanol, ethanol, n-octanol, DMSO, THF, toluene, benzene, acetonitrile, DMF, CH_2Cl_2 and hexane. It was revealed that all of the triazole derivatives absorb light in the UV-Vis region. The current alkoxy-substituted 1, 4-diarylated 1, 2, 3-triazole derivatives demonstrated an emission wavelength lower than that for previously reported conjugate triazole molecular systems (Ahmed and Xiong, 2021; Torres et al., 2021; Zhang et al., 2017). The π - π^* transition is responsible for those

absorption bands (Wang et al., 2010). The absorption wavelengths of the symmetric series were monitored to increase with raising the alkoxy chain length. This indicates that the excited state of the shorter alkoxy chain substituted triazole is lower than the excited state of the longer alkoxy chain substituted diarylated triazole. An increase in the UV-Vis absorption wavelength (Bathochromic shift) associated with a drop in fluorescence emission maxima was monitored when the length of the aliphatic tail was increased. Solvatochromic and solvatofluorochromic characteristics were shown in the UV-Vis absorption and fluorescence wavelengths in various solvents of different polarities. As the polarity of the solvent increases, a rise in the maximum wavelength was monitored in the absorption (positive solvatochromism) and fluorescence (positive solvatofluorochromism) spectra. In addition, it was found that the fluorescence quantum yield decreases when the length of the aliphatic alkoxy chain increases.

3.3. Gelation properties

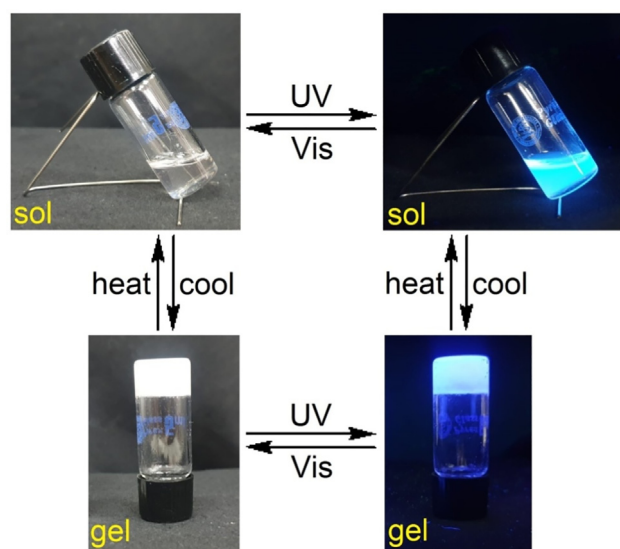
The nanofibrous architectures of self-assembled π -conjugated molecular systems have been reported with various characteristics in comparison to these π -conjugate building blocks themselves. Emission has been a critical character with the ability to display a key responsiveness to the surrounding environment. For example, emissive structures have a significant modulation effects on wavelength and intensity of emission as a result of forming supramolecular systems. Therefore, emissive assemblies are priceless materials for detecting a variety of analytes (Lin et al., 2019; Lin et al., 2017; Sasaki et al., 2020). In the current study, no gelation was monitored for the synthesized tetrahexyl-substituted triazole adduct **3a**. The prepared alkoxy-substituted 1, 4-diarylated 1, 2, 3-triazole gelators composed of four terminal alkoxy groups of high flexibility separated with the rigid bis(triazole)aryl core responsible for π -stacking. Aggregation of these alkoxy-substituted 1, 4-diarylated 1, 2, 3-triazole molecular gelators provide three dimensional entanglements of nanofibrous network that can be controlled by crystal formation and degree of solubility. Gelators **3a-c** are soluble in some solvents upon heating. Upon dissolution of compounds **3a-c** in solvents by heating, and then cooling to ambient temperature, a solid-like organogel was formed and monitored by the "stable to inversion" method as illustrated in Fig. 1. The gel formation of adducts **3a-c** was studied in several organic solvents. The values of critical gel concentration for gelator **3b** were monitored to be solvent-dependent ranging between 1.84 and 9.28 mM. Com-



Scheme 1 Synthesis of triazolo-based organogelators **3a-c**.

Table 1 Absorption and fluorescence maxima in various solvents.

Solvent	λ (nm)					
	3a		3b		3c	
	Abs.	Em.	Abs.	Em.	Abs.	Em.
<i>THF</i>	285	326	287	316	289	307
<i>DMSO</i>	291	323	290	313	294	308
<i>Ethanol</i>	290	325	293	315	297	309
<i>n-Propanol</i>	288	329	286	318	292	308
<i>n-Octanol</i>	286	327	289	315	294	305
<i>Toluene</i>	279	328	281	316	289	299
<i>Benzene</i>	281	328	285	319	290	301
Ethylacetate	286	331	287	320	285	309
1,2-Dichloroethane	288	326	292	316	298	315
<i>Acetonitrile</i>	289	327	290	316	290	318
<i>DMF</i>	287	329	288	319	296	321
CH_2Cl_2	276	315	280	305	285	299
$CHCl_3$	275	314	282	303	286	294
<i>Hexane</i>	273	312	278	302	280	297

**Fig. 1** Thermal and emission reversibility of gel **3b** (*n*-octanol) monitored by the stable to inversion approach under ultraviolet (UV) and visible (Vis) lights.

Compound **3b** shows a considerable capacity to gelate various organic solvents such as ethylacetate, chloroform, acetonitrile and *n*-octanol. However, adduct **3b** was partially gelled in other solvents such as *n*-propanol and toluene, hexane and displayed no gelation in other solvents such as dichloromethane, THF, ethanol, 1,2-dichloroethane, DMF, DMSO and benzene. The gelation study of adducts **3a-c** in various solvents is presented in Table 2. Compound **3a** demonstrated low solubility in organic solvents. Thus, it precipitates in many solvents. On the other hand, compound **3c** demonstrated a very high solubility in organic solvents. Thus, it is displayed formation of solutions in many solvents. All organogels formed in organic solvents are either colorless or white non-flowing organogels. The sol-gel switchable course was thermally reversible. The synthesized organogelators demonstrated similar photo-

Table 2 Gelation screening of tetraalkoxylated 1, 4-diarylated 1, 2, 3-triazole organogelators **3a-c** in various solvents.

Solvent	3a	3b	3c
<i>THF</i>	P	S	S
<i>DMSO</i>	S	S	S
<i>Ethanol</i>	P	P	S
<i>n-Propanol</i>	PG	PG	PG
<i>n-Octanol</i>	PG	G (1.84 mM)	G (5.02 mM)
<i>Toluene</i>	PG	PG	PG
<i>Benzene</i>	P	P	P
Ethylacetate	PG	G (3.51 mM)	PG
1,2-Dichloroethane	P	P	S
<i>Acetonitrile</i>	PG	G (3.78 mM)	PG
<i>DMF</i>	S	S	S
CH_2Cl_2	S	S	S
$CHCl_3$	PG	G (9.28 mM)	PG
<i>Hexane</i>	P	P	P

S: sol; G: gel; PG: partial gel; P: ppt; Critical gel content (mM) is displayed between a parenthesis.

physical properties similar to those monitored in their respective solution-based photophysical properties. The alkyl chains are non-polar moieties comprising only single bonds with carbon and hydrogen atoms. Therefore, the interactions among alkyl chains are comparatively weak London/Dispersion van der Waals forces, which usually increase as the length of the alkyl chain increases as a result of increasing the molecule surface area. Thus, compounds **3b-c** with longer alkyl chains demonstrated an improved organogel formation as compared to compound **3a** with the shorter length of alkyl chains.

As shown in Fig. 2, the blue shifting of the fluorescence maxima for the gel state of **3b** in comparison to that in an ethyl alcohol solution (diluted) indicates the presence of H-aggregates in the supramolecular organogel (Lin et al., 2019). It has been shown that H-aggregate systems have a propensity to form two-dimensional nanofibers due to the intermolecular

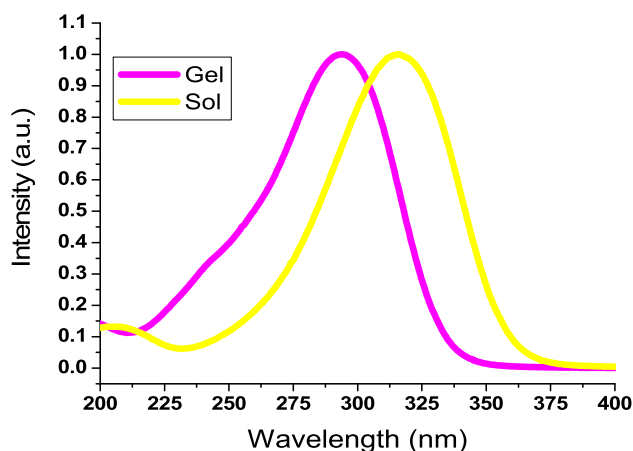


Fig. 2 Normalized emission spectra of **3b** in solution (*n*-octanol; 1.09×10^{-5} mol L⁻¹) and organogel states.

van der Waals interactions of tetraalkoxyls as well as intermolecular π -stacks of rigid bis(triazole)aryl core.

Table 3 shows both fluorescence wavelength and quantum yield of **3a-c** in solution and organogel (or partial organogel) states. The gel demonstrated different fluorescence wavelengths in comparison to the respective sol states of the same gelator. In *n*-octanol, the fluorescence of **3b** at 315 nm for the sol state shifts to 293 nm for the organogel state. The partial gel demonstrated lower shifting in the fluorescence wavelength in comparison to the completely gel formation case. For **3a** and **3b**, the quantum efficiency was observed to improve in the organogel state in comparison to the solution state (Altoom 2021; Radwan and Makhlof, 2021).

The thermal stability of the synthesized triazole **3b** in *n*-octanol was explored by investigating the critical gel concentration reliant gel \rightarrow sol conversion as illustrated in Fig. 3. The organogel melting point was recorded to rise between 41 and 55 °C with raising the gelator concentration between 1.84 and 14.00 mmol/L. This improved thermostability can be ascribed to the high crowd of the gelator molecules in the fiber bulk. However, the organogel melting point decreased when the gelator concentration increased to a value above 14.00 mmol/L. These increments monitored for the gel \rightarrow sol transition temperature could be attributed to increasing the 1D fiber aggregation imparting this fiber higher flexibility to result in nanofibrous entanglement, and accordingly rising the transition temperature.

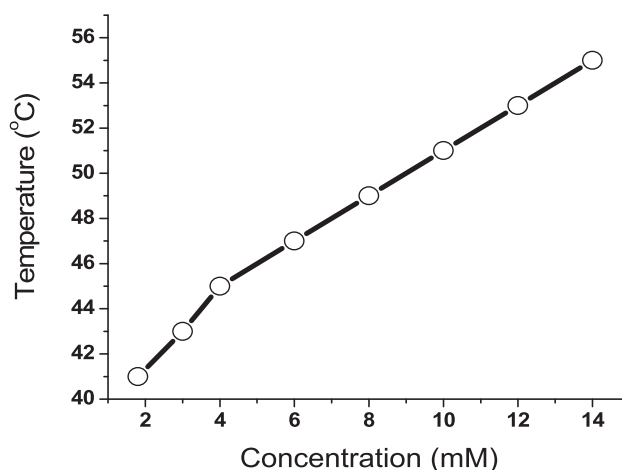


Fig. 3 Gel \rightarrow sol transition temperature against the organogelator (**3b**) quantity in *n*-octanol.

To investigate the gel \rightarrow sol reversibility, the temperature-dependent transition was explored (Fig. 4). The non-flowing solid-like gel was heated to boiling (~ 195 °C for *n*-octanol) until a transparent solution formed. The collapsing temperature of the gel was reported. The solution was then placed on a flat surface to settle for a few minutes at room temperature (~ 25 °C) to allow the organogel to regenerate as confirmed by the “stable to inversion” approach. This procedure was repeated to designate no change occurred in the gel \rightarrow sol switching temperature proving good reversibility.

3.4. Morphological properties

Using SEM analysis, the surface morphologies of the triazole gelators **3a-c** were examined to analyze the roles of π -stacks and van der Waals forces in guiding their formation. The self-assembled intertwined nanofibers were found to be well-ordered and homogeneous. SEM images were used to study the aggregation morphology of gelator **3b** dried xerogel (Fig. 5). Sample of dried xerogel from gelator **3b** was transferred to a glass slide and examined using SEM to demonstrate three dimensional entangled assemblies accounting for the immobilization of solvent molecules. Examination of SEM images displayed higher order of nanofibrous assemblies with the ability to bundle and generate strong and highly porous entanglements indicating highly directed intermolecular attraction forces. Nanofibers with diameters of 250–320 nm and few

Table 3 Fluorescence maxima [λ_{em} (nm)] and quantum yields [Φ_F] of **3a-c** in solution (1.09×10^{-5} mol L⁻¹) and gelation (partial gelation) states.

Solvent	3a				3b				3c			
	sol		gel		sol		gel		sol		gel	
	λ_{em}	Φ_F^*	λ_{em}	Φ_F	λ_{em}	Φ_F	λ_{em}	Φ_F	λ_{em}	Φ_F^*	λ_{em}	Φ_F
<i>n</i> -Propanol	329	0.61	307	0.65	318	0.58	297	0.63	308	0.36	279	0.41
<i>n</i> -Octanol	327	0.45	305	0.55	315	0.41	293	0.47	305	0.4	276	0.45
Toluene	328	0.43	306	0.44	316	0.39	290	0.44	299	0.37	268	0.42
Ethylacetate	331	0.52	300	0.56	320	0.43	291	0.55	309	0.35	277	0.47
Acetonitrile	327	0.4	308	0.59	316	0.52	294	0.63	318	0.3	275	0.55
CHCl ₃	314	0.37	295	0.45	303	0.4	281	0.56	294	0.22	266	0.38

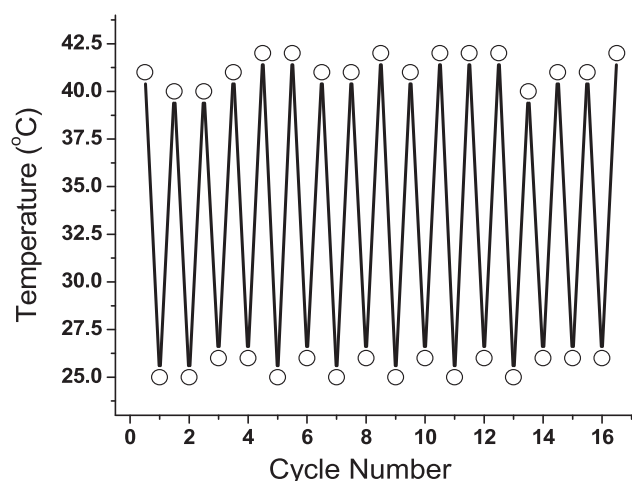


Fig. 4 Temperature-dependent sol-to-gel-to-sol reversibility without fatigue for **3b**.

micrometres long were monitored in the SEM micrographs of **3b** from *n*-octanol. The self-assembly of **3b** creates nanofibers via immobilization of organic solvents. When it comes to gelators, the presence of lengthy alkoxy groups has been observed as a key component in improving their stability.

3.5. Cytotoxicity measurements

Compounds **3a-c** were tested for cytotoxicity *in vitro* to determine the viability of certain BJ1 skin fibroblast cells exposed to these triazoles. Compounds **3a** and **3b** did not seem to affect on the cell proliferation. However, compound **3c** begins to lose its viability to result in 91.33 % viable cells. Because organic chemicals tend to precipitate out of solution, there is less room for cell growth, resulting in a drop in cell numbers. The current alkoxy-substituted 1, 4-diarylated 1, 2, 3-triazoles, as a consequence of these findings, are clearly harmless compounds. Thus, they can be potentially used for drug delivery applications. The antibacterial properties were also examined against *S. aureus* and *E. coli* to show acceptable antibacterial activity

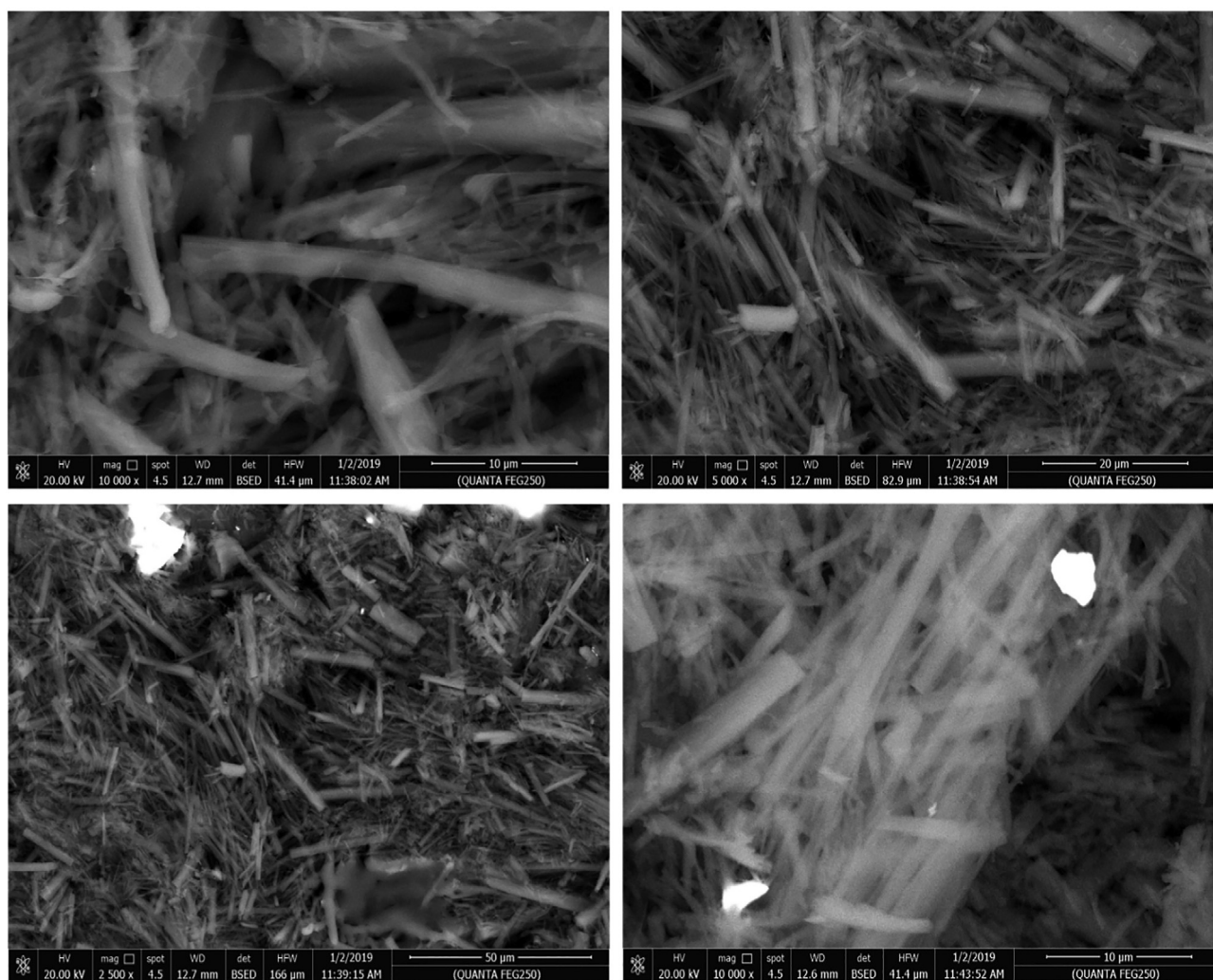


Fig. 5 SEM micrographs of dried xerogel generated from gelator **3b** in *n*-octanol.

Table 4 Antibacterial activity (Reduction %) of the synthesized triazoles.

Gelator	<i>E. coli</i>	<i>S. aureus</i>
3a	15 ± 1.2	13 ± 1.0
3b	19 ± 1.4	15 ± 1.1
3c	23 ± 1.3	16 ± 1.0

as shown in Table 4. However, the antibacterial activity decreased with raising the alkoxy chain length. Thus, the best antibacterial performance was monitored for compound **3a**.

Antimicrobial activity of nitrogen-containing heterocyclic compounds has been observed (Heravi and Zadsirjan, 2020; Zhang et al., 2010). The class of nitrogen-containing heterocyclic triazoles is especially intriguing because of its intrinsic biological activity (Gondru et al., 2021) and considerable utility as molecular building blocks in synthetic transformations (Patil et al., 2020; Phatak et al., 2020). Thus, scientists are now working to create novel functionalized triazole derivatives and investigate their biological effects. However, a little research studies have been reported on the synthesis of antibacterial triazoles (Nalawade et al., 2019; Yadav et al., 2018). Moreover, the development of triazole-based fluorescent organogels has not been described yet. The synthesis of innovative compounds with biological has been significant (Aragón-Muriel et al., 2021; Hernández-Romero et al., 2021; Ríos-Malvárez et al., 2021; Rufino-Felipe et al., 2021). Several low molecular mass organogels have recently been reported to be effective antibacterial and drug delivery materials that are not cytotoxic (Esposito et al., 2018; Rowley et al., 2020). Bioimaging, antimicrobials, and drug delivery systems all benefit from the newly synthesized triazole-based fluorescent low molecular mass organogels.

4. Conclusion

New series of alkoxy-substituted 1, 4-diarylated 1, 2, 3-triazoles able to generate nanofibrous self-assembled packing were introduced by the versatile and standard simple CuAAC reaction. The existence of 1, 2, 3-triazole heterocyclic ring was found to promote well self-assembled supramolecular architectures by gelating organic solvents. The appropriate molecular combination of 1, 2, 3-triazole heterocyclic ring, aryl rings, and terminal alkoxy chains allowed for the formation of supramolecular architectures. We studied their distinctive self-assembly of these alkoxy-substituted 1, 4-diarylated 1, 2, 3-triazole structures into nanofibrous (250–320 nm) architectures as reported by SEM analysis. The formation of extended nanofibers could be attributed to van der Waals of long alkoxy groups and π -stacking of aryl rings. The current triazole gelators were monitored to non-cytotoxic and exhibit an acceptable antibacterial activity.

Acknowledgements

Princess Nourah bint Abdulrahman University Researchers Supporting Project number (PNURSP2022R122), Princess Nourah bint Abdulrahman University, Riyadh, Saudi Arabia.

Competing Interests

All the authors hereby declare that they do not have any conflict of interest about this manuscript.

Data availability

All relevant data are within the manuscript and available from the corresponding author upon request.

Compliance with ethical standards

Conflict of interest

The authors declare that they have no conflict of interest.

Ethical approval

Not applicable.

Consent to participate

All authors were participated in this work.

Consent to publish

All authors agree to publish.

References

- Abumelha, H.M., Al-Fahemi, J.H., Althagafi, I., Bayazeed, A.A., Al-Ahmed, Z.A., Khedr, A.M., El-Metwaly, N., 2020. Deliberate-characterization for Ni (II)-Schiff base complexes: promising in-vitro anticancer feature that matched MOE docking-approach. *J. Inorg. Organomet. Polym. Mater.* 30 (9), 3277–3293.
- Afzali, E., Mirjafary, Z., Akbarzadeh, A., Saeidian, H., 2021. Complexation of copper ion-containing immobilized ionic liquid in designed hierarchical-functionalized layered double hydroxide nanoreactor for azide–alkyne cycloaddition reaction. *Inorg. Chem. Commun.* 132, 108858.
- Agarwal, D.S., Singh, R.P., Jha, P.N., Sakhuja, R., 2020. Fabrication of deoxycholic acid tethered α -cyanostilbenes as smart low molecular weight gelators and AIEE probes for bio-imaging. *Steroids* 160, 108659.
- Ahmed, F., Xiong, H., 2021. Recent developments in 1, 2, 3-triazole-based chemosensors. *Dyes Pigm.* 185, 108905.
- Aldalbahi, A., Periyasami, G., Alrehaili, A., 2021. Synthesis of high molar extinction coefficient push–pull tricyanofuran-based disperse dyes: Biological activity and dyeing performance. *New J. Chem.* 45 (4), 2208–2216.
- Alsoliemy, A., Alrefaei, A.F., Almeahadi, S.J., Almeahadi, S.J., Hossan, A., Khalifa, M.E., El-Metwaly, N.M., 2021. Synthesis, characterization and self-assembly of new cholesteryl-substituted sym-tetrazine: Fluorescence, gelation and mesogenic properties. *J. Mol. Liq.* 342, 117543.
- Altoom, N.G., 2021. Synthesis and characterization of novel fluoroterphenyls: self-assembly of low-molecular-weight fluorescent organogel. *Luminescence* 36 (5), 1285–1299.
- Aragón-Muriel, A., Liscano, Y., Morales-Morales, D., Polo-Cerón, D., Oñate-Garzón, J., 2021. A study of the interaction of a new benzimidazole schiff base with synthetic and simulated membrane models of bacterial and mammalian membranes. *Membranes* 11 (6), 449.
- Bhardwaj, V., Ballabh, A., 2022. A series of multifunctional pivalamide based Low Molecular Mass Gelators (LMOGs) with potential applications in oil-spill remediation and toxic dye removal. *Colloids Surf. A: Physicochem. Eng. Asp.* 632, 127813.
- Díaz, D.D., Rajagopal, K., Strable, E., Schneider, J., Finn, M.G., 2006. “Click” chemistry in a supramolecular environment: stabi-

- lization of organogels by Copper (I)-catalyzed azide-alkyne [3 + 2] cycloaddition. *J. Am. Chem. Soc.* 128 (18), 6056–6057.
- Esposito, C.L., Kirilov, P., Roullin, V.G., 2018. Organogels, promising drug delivery systems: an update of state-of-the-art and recent applications. *J. Control. Release* 271, 1–20.
- Fakhrutdinov, A.N., Karlinskii, B.Y., Minyaev, M.E., Ananikov, V. P., 2021. Unusual Effect of Impurities on the Spectral Characterization of 1, 2, 3-Triazoles Synthesized by the Cu-Catalyzed Azide-Alkyne Click Reaction. *J. Org. Chem.* 86 (17), 11456–11463.
- Fernandes, C.M., Alvarez, L.X., dos Santos, N.E., Barrios, A.C.M., Ponzio, E.A., 2019. Green synthesis of 1-benzyl-4-phenyl-1H-1, 2, 3-triazole, its application as corrosion inhibitor for mild steel in acidic medium and new approach of classical electrochemical analyses. *Corros. Sci.* 149, 185–194.
- Gholampour, M., Ranjbar, S., Edraki, N., Mohabbati, M., Firuzi, O., Khoshneviszadeh, M., 2019. Click chemistry-assisted synthesis of novel aminonaphthoquinone-1, 2, 3-triazole hybrids and investigation of their cytotoxicity and cancer cell cycle alterations. *Bioorg. Chem.* 88, 102967.
- Ghosh, K., Panja, S., 2015. Coumarin-based supramolecular gelator: a case of selective detection of F⁻ and HP 2 O 7 3-. *RSC Adv.* 5 (16), 12094–12099.
- Gondru, R., Kanugala, S., Raj, S., Kumar, C.G., Pasupuleti, M., Banothu, J., Bavantula, R., 2021. 1, 2, 3-triazole-thiazole hybrids: Synthesis, in vitro antimicrobial activity and antibiofilm studies. *Bioorg. Med. Chem. Lett.* 33, 127746.
- Goyal, H., Pachisia, S., Gupta, R., 2020. Systematic design of a low-molecular-weight gelator and its application in the sensing and retention of residual antibiotics. *Cryst. Growth Des.* 20 (9), 6117–6128.
- Gu, X., Guo, S., Wang, G., 2020. Preparation, hydrogen bonding and properties of polyurethane elastomers with 1, 2, 3-triazole units by click chemistry. *Polym. Eng. Sci.* 60 (12), 3270–3280.
- Güzel, E., 2019. Dual-purpose zinc and silicon complexes of 1, 2, 3-triazole group substituted phthalocyanine photosensitizers: synthesis and evaluation of photophysical, singlet oxygen generation, electrochemical and photovoltaic properties. *RSC Adv.* 9 (19), 10854–10864.
- Heravi, M.M., Zadsirjan, V., 2020. Prescribed drugs containing nitrogen heterocycles: An overview. *RSC Adv.* 10 (72), 44247–44311.
- Hernández-Romero, D., Rosete-Luna, S., López-Monteon, A., Chávez-Piña, A., Pérez-Hernández, N., Marroquín-Flores, J., Cruz-Navarro, A., Pesado-Gómez, G., Morales-Morales, D., Colorado-Peralta, R., 2021. First-row transition metal compounds containing benzimidazole ligands: An overview of their anticancer and antitumor activity. *Coord. Chem. Rev.* 439, 213930.
- Horsten, T., de Jong, F., Theunissen, D., Van der Auweraer, M., Dehaen, W., 2021. Synthesis and spectroscopic properties of 1, 2, 3-triazole BOPAHY dyes and their water-soluble triazolium salts. *J. Org. Chem.* 86 (19), 13774–13782.
- Huang, Y., Liu, S., Xie, Z., Sun, Z., Chai, W., Jiang, W., 2018. Novel 1, 2, 3-triazole-based compounds: Iodo effect on their gelation behavior and cation response. *Front. Chem. Sci. Eng.* 12 (2), 252–261.
- Huang, Y., Zhang, Y., Yuan, Y., Cao, W., 2015. Organogelators based on iodo 1, 2, 3-triazole functionalized with coumarin: properties and gelator-solvent interaction. *Tetrahedron* 71 (14), 2124–2133.
- Lakdusinghe, M., Abbaszadeh, M., Mishra, S., Sengottuvelu, D., Wijayapala, R., Zhang, S., Benasco, A.R., Gu, X., Morgan, S.E., Wipf, D.O., Kundu, S., 2021. Nanoscale Self-Assembly of Poly (3-hexylthiophene) Assisted by a Low-Molecular-Weight Gelator toward Large-Scale Fabrication of Electrically Conductive Networks. *ACS Appl. Nano Mater.* 4 (8), 8003–8014.
- Lin, Q., Guan, X.W., Fan, Y.Q., Wang, J., Liu, J., Yao, H., Zhang, Y.M., Wei, T.B., 2019. A tripodal supramolecular sensor to successively detect picric acid and CN⁻ through guest competitive controlled AIE. *New J. Chem.* 43 (4), 2030–2036.
- Lin, Q., Liu, L., Zheng, F., Mao, P.P., Liu, J., Zhang, Y.M., Yao, H., Wei, T.B., 2017. A novel water soluble self-assembled supramolecular sensor based on pillar [5] arene for fluorescent detection CN⁻ in water. *Tetrahedron* 73 (35), 5307–5310.
- Mandegani, F., Zali-Boeini, H., Khayat, Z., Scopelliti, R., 2020. A smart low molecular weight gelator for the triple detection of copper (II), mercury (II), and cyanide ions in water resources. *Talanta* 219, 121237.
- Mellerup, S.K., Wang, S., 2019. Boron-based stimuli responsive materials. *Chem. Soc. Rev.* 48 (13), 3537–3549.
- Morris, J., Bietsch, J., Bashaw, K., Wang, G., 2021. Recently developed carbohydrate based gelators and their applications. *Gels* 7 (1), 24.
- Moulin, E., Faour, L., Carmona-Vargas, C.C., Giuseppone, N., 2020. From Molecular Machines to Stimuli-Responsive Materials. *Adv. Mater.* 32 (20), 1906036.
- Naim, K., Sahoo, S.C., Venugopalan, P., Neelakandan, P., 2021. Remarkable Self-Assembly of Salicylideneimine-Boron Complexes into Plastic Crystals and Organogels. *Cryst. Growth Des.* 21 (7), 3798–3806.
- Nalawade, J., Shinde, A., Chavan, A., Patil, S., Suryavanshi, M., Modak, M., Choudhari, P., Bobade, V.D., Mhaske, P.C., 2019. Synthesis of new thiazolyl-pyrazolyl-1, 2, 3-triazole derivatives as potential antimicrobial agents. *Eur. J. Med. Chem.* 179, 649–659.
- Oh, J., Baek, D., Lee, T.K., Kang, D., Hwang, H., Go, E.M., Jeon, I., You, Y., Son, C., Kim, D., Whang, M., 2021. Dynamic multimodal holograms of conjugated organogels via dithering mask lithography. *Nat. Mater.* 20 (3), 385–394.
- Patil, P.S., Kasare, S.L., Haval, N.B., Khedkar, V.M., Dixit, P.P., Rekha, E.M., Sriram, D., Haval, K.P., 2020. Novel isoniazid embedded triazole derivatives: Synthesis, antitubercular and antimicrobial activity evaluation. *Bioorg. Med. Chem. Lett.* 30 (19) 127434.
- Phatak, P.S., Bakale, R.D., Kulkarni, R.S., Dhupal, S.T., Dixit, P.P., Krishna, V.S., Sriram, D., Khedkar, V.M., Haval, K.P., 2020. Design and synthesis of new indanol-1, 2, 3-triazole derivatives as potent antitubercular and antimicrobial agents. *Bioorg. Med. Chem. Lett.* 30 (22) 127579.
- Radwan, A.S., Makhlof, M.M., 2021. Synthesis, characterization, and self-assembly of fluorescent fluorine-containing liquid crystals. *Luminescence* 36 (7), 1751–1760.
- Rastogi, P., Kandasubramanian, B., 2019. Breakthrough in the printing tactics for stimuli-responsive materials: 4D printing. *Chem. Eng. J.* 366, 264–304.
- Raymond, D.M., Abraham, B.L., Fujita, T., Watrous, M.J., Toriki, E. S., Takano, T., Nilsson, B.L., 2019. Low-molecular-weight supramolecular hydrogels for sustained and localized in vivo drug delivery. *ACS Appl. Bio Mater.* 2 (5), 2116–2124.
- Reddy, S.M.M., Dorishetty, P., Augustine, G., Deshpande, A.P., Ayyadurai, N., Shanmugam, G., 2017. A low-molecular-weight gelator composed of pyrene and fluorene moieties for effective charge transfer in supramolecular ambidextrous gel. *Langmuir* 33 (47), 13504–13514.
- Rios-Malvárez, Z.G., Cano-Herrera, M.A., Dávila-Becerril, J.C., Mondragón-Solórzano, G., Ramírez-Apan, M.T., Morales-Morales, D., Barroso-Flores, J., Santillán-Benítez, J.G., Unnamatla, M. B., Garcia-Eleno, M.A., González-Rivas, N., 2021. Synthesis, characterization and cytotoxic activity evaluation of 4-(1, 2, 3-triazol-1-yl) salicylic acid derivatives. *J. Mol. Struct.* 1225, 129149.
- Ross, D.A., Findlay, J.A., Vasdev, R.A., Crowley, J.D., 2021. Can 2-Pyridyl-1, 2, 3-triazole “Click” Ligands be Used to Develop Cu (I)/Cu (II) Molecular Switches? *ACS Omega* 6 (44), 30115–30129.
- Rowley, J.V., Wall, P., Yu, H., Tronci, G., Devine, D.A., Vernon, J.J., Thornton, P.D., 2020. Antimicrobial dye-conjugated polyglobulide-based organogels. *ACS Appl. Polym. Mater.* 2 (7), 2927–2933.
- Rufino-Felipe, E., Colorado-Peralta, R., Reyes-Márquez, V., Valdés, H., Morales-Morales, D., 2021. Fluorinated-NHC transition metal

- complexes: leading characters as potential anticancer metallodrugs. *Anti-Cancer Agents Med. Chem.* 21 (8), 938–948.
- Sasaki, Y., Ito, S., Zhang, Z., Lyu, X., Takizawa, S.Y., Kubota, R., Minami, T., 2020. Supramolecular sensor for astringent procyanidin C1: Fluorescent artificial tongue for wine components. *Chem. Eur. J.* 26 (69), 16236–16240.
- Sharma, N., Gupta, M., Chowhan, B., Frontera, A., 2021a. Magnetically separable nanocatalyst (IL@ CuFe₂O₄-L-Tyr-TiO₂/TiT-CIL): Preparation, characterization and its applications in 1, 2, 3-triazole synthesis and in photodegradation of MB. *J. Mol. Struct.* 1224, 129029.
- Sharma, P., Chen, A., Wang, D., Wang, G., 2021b. Synthesis and Self-Assembling Properties of Peracetylated β -1-Triazolyl Alkyl D-Glucosides and D-Galactosides. *Chemistry* 3 (3), 935–958.
- Sun, Y., Wang, Y.X., Wu, M., Yuan, W., Chen, Y., 2017. p-Quaterphenylene as an Aggregation-Induced Emission Fluorogen in Supramolecular Organogels and Fluorescent Sensors. *Chem. Asian J.* 12 (1), 52–59.
- Tang, H., Duan, X., Feng, X., Liu, L., Wang, S., Li, Y., Zhu, D., 2009. Fluorescent DNA–poly (phenylenevinylene) hybrid hydrogels for monitoring drug release. *Chem. Commun.* 6, 641–643.
- Tao, Y., Wang, Q., Ao, L., Zhong, C., Yang, C., Qin, J., Ma, D., 2010. Highly efficient phosphorescent organic light-emitting diodes hosted by 1, 2, 4-triazole-cored triphenylamine derivatives: relationship between structure and optoelectronic properties. *J. Phys. Chem. C* 114 (1), 601–609.
- Tautz, M., Saldias, C., Lozano-Gorrin, A.D., Díaz, D.D., 2019. Use of a bis-1, 2, 3-triazole gelator for the preparation of supramolecular metallogels and stabilization of gold nanoparticles. *New J. Chem.* 43 (35), 13850–13856.
- Torres, J.G.G., Becerra-Buitrago, A., García-Sánchez, L.C., García-Eleno, M.A., Unnamatla, M.B., Cuevas-Yañez, E., 2021. Azide-Alkyne Cycloaddition Catalyzed by a Glucose/Benedict Reagent System. <https://doi.org/10.3390/ecsoc-25-11634>.
- van Hilst, Q.V., Lagesse, N.R., Preston, D., Crowley, J.D., 2018. Functional metal complexes from CuAAC “click” bidentate and tridentate pyridyl-1, 2, 3-triazole ligands. *Dalton Trans.* 47 (4), 997–1002.
- Vishnevetskii, D.V., Mekhtiev, A.R., Perevozova, T.V., Averkin, D. V., Ivanova, A.I., Khizhnyak, S.D., Pakhomov, P.M., 2020. l-Cysteine/AgNO₂ low molecular weight gelators: self-assembly and suppression of MCF-7 breast cancer cells. *Soft Matter* 16 (42), 9669–9673.
- Wang, J.L., Xiao, Q., Pei, J., 2010. Benzothiadiazole-based D– π -A– π -D organic dyes with tunable band gap: Synthesis and photophysical properties. *Org. Lett.* 12 (18), 4164–4167.
- Wang, Y., Versluis, F., Oldenhof, S., Lakshminarayanan, V., Zhang, K., Wang, Y., Wang, J., Eelkema, R., Guo, X., van Esch, J.H., 2018. Directed Nanoscale Self-Assembly of Low Molecular Weight Hydrogelators Using Catalytic Nanoparticles. *Adv. Mater.* 30 (21), 1707408.
- Wu, C.S., Chen, Y., 2010. Copoly (p-phenylene)s containing bipolar triphenylamine and 1, 2, 4-triazole groups: Synthesis, optoelectronic properties, and applications. *J. Polym. Sci. A: Polym. Chem.* 48 (24), 5727–5736.
- Xu, Z., Cheng, G., Zhu, S., Lin, Q., Yang, H., 2018. Nitrogen-rich salts based on the combination of 1, 2, 4-triazole and 1, 2, 3-triazole rings: a facile strategy for fine tuning energetic properties. *J. Mater. Chem. A* 6 (5), 2239–2248.
- Yadav, P., Lal, K., Kumar, L., Kumar, A., Kumar, A., Paul, A.K., Kumar, R., 2018. Synthesis, crystal structure and antimicrobial potential of some fluorinated chalcone-1, 2, 3-triazole conjugates. *Eur. J. Med. Chem.* 155, 263–274.
- Yang, H.K., Zhao, H., Yang, P.R., Huang, C.H., 2017. How do molecular structures affect gelation properties of supramolecular gels? Insights from low-molecular-weight gelators with different aromatic cores and alkyl chain lengths. *Colloids Surf. A: Physicochem. Eng. Asp.* 535, 242–250.
- Yang, Y., Mori, A., Hashidzume, A., 2019. Emission properties of diblock copolymers composed of poly (ethylene glycol) and dense 1, 2, 3-triazole blocks. *Polymers* 11 (7), 1086.
- Zeng, L., Lin, X., Li, P., Liu, F.Q., Guo, H., Li, W.H., 2021. Recent advances of organogels: from fabrications and functions to applications. *Prog. Org. Coat.* 159, 106417.
- Zhang, W., Zhang, Z., Zhao, S., Hong, K.H., Zhang, M.Y., Song, L., Yu, F., Luo, G., He, Y.P., 2021. Pyromellitic-based low molecular weight gelators and computational studies of intermolecular interactions: a potential additive for lubricant. *Langmuir* 37 (9), 2954–2962.
- Zhang, X., Lu, R., Jia, J., Liu, X., Xue, P., Xu, D., Zhou, H., 2010. Organogel based on β -diketone-boron difluoride without alkyl chain and H-bonding unit directed by optimally balanced π – π interaction. *Chem. Commun.* 46 (44), 8419–8421.
- Zhang, X., Yan, X., Zhang, B., Wang, R., Guo, S., Peng, S., 2019. Mono- and dinuclear palladium (II) complexes incorporating 1, 2, 3-triazole-derived mesoionic carbenes: syntheses, solid-state structures and catalytic applications. *Transit. Met. Chem.* 44 (1), 39–48.
- Zhang, Y., He, Y., Wojtas, L., Shi, X., Guo, H., 2020. Construction of supramolecular organogel with circularly polarized luminescence by self-assembled guanosine octamer. *Cell Rep. Phys. Sci.* 1, (10) 100211.
- Zhang, Y.C., Jin, R., Li, L.Y., Chen, Z., Fu, L.M., 2017. Study on the Fluorescent Activity of N2-Indolyl-1, 2, 3-triazole. *Molecules* 22 (9), 1380.
- Zych, D., Slodek, A., Zimny, D., Golba, S., Malarz, K., Mrozek-Wilczkiewicz, A., 2019. Influence of the substituent D/A at the 1, 2, 3-triazole ring on novel terpyridine derivatives: synthesis and properties. *RSC Adv.* 9 (29), 16554–16564.